U(1)′ dark matter

David E. Brahm and Lawrence J. Hall
Physics Department, University of California, Berkeley, California 94720
and Theoretical Physics Group, Lawrence Berkeley Laboratory,
1 Cyclotron Road, Berkeley, California 94720
(Received 10 October 1989)

We consider models with a gauged U(1)′, to which is coupled a fermionic standard-model singlet ψ. If ψ's close the Universe, a Lee-Weinberg calculation gives the four-fermion coupling G' from the mass m_ψ. We can then calculate the germanium scattering cross section as a function of m_ψ. The results are nearly model independent and close to experimental limits for $10\,\mathrm{GeV} \leq m_\psi \leq 100\,\mathrm{GeV}$. In the region $400\,\mathrm{GeV} \leq m_\psi \leq 40\,\mathrm{TeV}$ the scattering cross section depends on $M_{Z'}$, and again approaches experimental limits if $M_{Z'} \leq 2\,\mathrm{TeV}$.

I. INTRODUCTION

In addition to their standard-model interactions, the known quarks and leptons may interact via gauge bosons somewhat heavier than the $W^\pm$ and Z^0. Such extra gauge bosons can be sought in particle accelerators, e.g., by direct production at e^+e^- or hadron colliders, or by measuring deviations from standard-model predictions for neutral-current and charged-current phenomena. In this paper we demonstrate that present and future dark-matter detectors provide powerful, indirect probes for a Z'. Furthermore, searches can cover a large mass range, $M_Z < M_{Z'} \leq 2\,\mathrm{TeV}$.

This probe rests on the assumption that the dark matter is a neutral Dirac fermion ψ, which interacts with ordinary matter only through the Z', with coupling strength

$$G' = \frac{\sqrt{2}}{8}\frac{(g_1')^2}{M_{Z'}^2} \ . \tag{1}$$

A freeze-out calculation gives a relic abundance for ψ of approximately

$$\Omega_\psi = \frac{(1/66\,\mathrm{TeV})^2}{\langle\sigma_A v\rangle h_0^2} = 1 \ , \tag{2}$$

where

$$\langle\sigma_A v\rangle \sim (G')^2 m_\psi^2 \quad (m_\psi < M_{Z'}) \ , \tag{3a}$$

$$\langle\sigma_A v\rangle \sim (g_1')^4/m_\psi^2 \quad (m_\psi > M_{Z'}) \ , \tag{3b}$$

and $h_0 = \frac{1}{2}$. Constraining $g_1' < \sqrt{4\pi}$ limits us to the region $1\,\mathrm{GeV} < m_\psi < 40\,\mathrm{TeV}$.

This dark matter could be directly seen by germanium[1,2] (or superconducting granule[3]) detectors, which register the nuclear recoil from an elastic collision between ψ and a nucleus. The coherent elastic scattering cross section from Z' exchange is

$$\sigma_{\mathrm{el}} \sim \frac{(G')^2 m_\psi^2 A^2}{(1 + m_\psi/M_{\mathrm{Ge}})^2} \ , \tag{4}$$

where A is the atomic weight and M_{Ge} is the mass of the nucleus. This is correct even for $m_\psi > M_{Z'}$, since the momentum transfer is low. Equations (2), (3), and (4) combine to give

$$\sigma_{\mathrm{el}} \sim \frac{1}{(1 + m_\psi/M_{\mathrm{Ge}})^2} \quad (m_\psi < M_{Z'}) \ , \tag{5a}$$

$$\sigma_{\mathrm{el}} \sim m_\psi^2/M_{Z'}^4 \quad (m_\psi > M_{Z'} > M_{\mathrm{Ge}}) \ . \tag{5b}$$

Thus, for $m_\psi < M_{Z'}$, σ_{el} is large and constant when $m_\psi < M_{\mathrm{Ge}}$, then drops as $1/m_\psi^2$ at larger values. σ_{el} increases again (as m_ψ^2) for $m_\psi > M_{Z'}$, so it is possible to get observable signals over large ranges of m_ψ and $M_{Z'}$. Our calculations show the most likely regions for observable signals are

(I) $10\,\mathrm{GeV} < m_\psi < 100\,\mathrm{GeV}$ $(m_\psi < M_{Z'})$,
(II) $400\,\mathrm{GeV} < m_\psi < 40\,\mathrm{TeV}$ $(m_\psi > M_{Z'})$.

In this Introduction we have argued that experiments searching for elastic scattering of dark-matter particles may allow for a probe of a new U(1)′ gauge interaction. After an overview of some U(1)′ models in Sec. II we calculate cross sections in Sec. III for both Dirac and Majorana fermions. The results for Dirac fermions (Secs. III A and III B) are close to experimental limits. In Secs. IV and V we look at additional model-dependent constraints, and our results are summarized in Sec. VI.

II. U(1)′ MODELS

A. A prototype U(1)′

The choice of a U(1)′ will affect our final result for σ_{el} by a small multiplicative factor Φ, generally in the range

$\frac{1}{2} \leq \Phi \leq \frac{3}{2}$ (though $\Phi \ll 1$ in cases of accidental cancellation of the proton and neutron charges). We choose in this subsection a prototype U(1)′, for which we take $\Phi \equiv 1$.

Consider $SO(10) \rightarrow SU(5) \otimes U(1)_X$. The SU(5) is taken to be the usual Georgi-Glashow model, and we break $U(1)_X$ at roughly the TeV scale with a Higgs field ϕ (from a $\overline{16}$). Our prototype U(1)′ is then just $U(1)_X$, whose normalized charge is

$$S^{(1)} = \sqrt{\tfrac{5}{8}}(B - L - \tfrac{4}{5}Y) \ . \tag{6}$$

In addition to the 15 standard-model Weyl spinors (Q, U^c, D^c, L, and E^c), the **16** of SO(10) contains an N^c which transforms under $SU(5) \otimes U(1)_X$ as $(\mathbf{1}, \sqrt{5/8})$. A term $\phi N^c N$ couples N^c to an SO(10) singlet N, giving rise to a Dirac fermion

$$\psi = \begin{pmatrix} \bar{N} \\ N^c \end{pmatrix} \ . \tag{7}$$

ψ is our dark-matter candidate, coupling to ordinary matter only through the exchange of a TeV-scale Z'.

We omit all couplings like $LN^c h^c$ which would make ψ unstable, by imposing some discrete symmetry (e.g., $N \rightarrow iN$, $N^c \rightarrow -iN^c$). One can view such an SO(10)-violating discrete symmetry two ways. The first is to simply accept the low-energy model as it stands, with Yukawa couplings

$$\mathcal{L} = QU^c h^c + QD^c h + LE^c h + \phi N^c N \tag{8}$$

and with the gauged $U(1)_X$, without worrying about grand-unified-theory (GUT) embeddings (or even supersymmetry). The second is to invoke the Hosotani breaking mechanism, in which Yukawa couplings do not maintain the expected relations, and may vanish by a discrete symmetry or for topological reasons.[4]

Another possibility we will consider, in the absence of the SO(10) singlet N, is that N^c forms a Majorana fermion. Since Majorana fermions only have axial-vector couplings, they are much harder to detect.

B. Other popular U(1)'s

Nothing in the calculations of Sec. III requires unification; however, in order to sample some other U(1)′ theories, we now consider several models which arise from E_6 unification.

When E_6 breaks down,

$$E_6 \rightarrow SO(10) \otimes U(1)_\Omega \rightarrow SU(5) \otimes U(1)_X \otimes U(1)_\Omega \ , \tag{9}$$

the known particles can be embedded in three different ways,[5] corresponding to Georgi-Glashow,[6] flipped,[7] and doubly flipped[8] SU(5) (see Table I), and in each case different symmetry-breaking mechanisms can lead to different low-energy U(1)′ symmetries. Any anomaly-free U(1)′ can be characterized as $\beta(B-L)+\lambda Y+\kappa P$, where P is a variant of Peccei-Quinn symmetry. $(B-L)$, Y, and P charges for particles in the **27** are shown in Table II.

Georgi-Glashow SU(5), broken by an adjoint Higgs field (or the Hosotani mechanism), has two leftover U(1) symmetries; we must choose one linear combination to be our U(1)′. String phenomenologists have three favorite choices, known variously in the literature as A, B, C (Ref. 9) or η, χ, I (Ref. 10) or Y''', Y'', Y' (Ref. 11). Model B (χ, Y'') is identical to our prototype $S^{(1)}$, discussed in the previous subsection. Model C (I, Y'), which we call $S^{(2)}$, is popular because the N^c can take a large Majorana mass and drive the neutrino-mass seesaw mechanism; in that case our ψ would have to consist of N (if Majorana), or of N and an E_6 singlet P (if Dirac). Model A [η, Y''', or Y_E (Ref. 12)], which we call $S^{(3)}$, is the only one which arises from Hosotani breaking of E_6 directly to the rank-5 group.

Flipped $SU(5) \otimes U(1)_X$ is broken to the standard model with Higgs fields in the $(\mathbf{10}, -1)$ and $(\overline{\mathbf{10}}, 1)$ representations. Depending on where these Higgs fields reside in E_6, they can leave different U(1)′ symmetries unbroken. If they come from **27** and $\overline{\mathbf{27}}$, they leave symmetry $S^{(4)}$, while if they come from a **78**, they leave $S^{(5)}$. Doubly flipped $SU(5) \otimes U(1)_X \otimes U(1)_\Omega$ is broken to the standard model by Higgs fields in the $(\mathbf{10}, -1, 1)$ and $(\overline{\mathbf{10}}, 1, -1)$ representations (from **27** and $\overline{\mathbf{27}}$), which leave yet another U(1)′ candidate, $S^{(6)}$.

Finally, we consider $S^{(7)} = B - L$, which comes, for example, from a Pati-Salam model.[13] Our seven popular U(1)′'s, with their $[\beta, \lambda, \kappa]$ values, particle charges, and normalizations, are listed in Table II.

III. CROSS-SECTION CALCULATIONS

A. A light Dirac fermion

In this subsection we predict the germanium scattering cross section for a Dirac fermion with $m_\psi \ll \frac{1}{2}M_{Z'}$. This is the most interesting case, since our results are nearly model independent and close to experimental limits. ψ must consist of two Weyl spinors of different U(1)′ charges; otherwise the calculations of Sec. III C apply. Under our various candidate symmetries, we could take

TABLE I. Particle assignments for the **27** of E_6.

27	$\rightarrow$	$[(\mathbf{10}, -1, 1)$	$\oplus$	$(\overline{\mathbf{5}}, 3, 1)$	$\oplus$	$(1, -5, 1)]$	$\oplus$	$[(\overline{\mathbf{5}}, -2, -2)$	$\oplus$	$(\mathbf{5}, 2, -2)]$	$\oplus$	$[(1, 0, 4)]$
G-G:		Q, U^c, E^c		D^c, L		N^c		B^c, h		B, h^c		N
1-Flip:		Q, U^c, N^c		U^c, L		E^c		B^c, h^c		B, h		N
2-Flip:		Q, B^c, N		D^c, h^c		N^c		U^c, h		B, L		E^c

TABLE II. Charges for candidate U(1)′ symmetries.

S	β	λ	κ	Q	D^c	U^c	L	E^c	N^c	h	h^c	B	B^c	N	Norm
$B-L$	1	0	0	$\frac{1}{3}$	$-\frac{1}{3}$	$-\frac{1}{3}$	-1	1	1	0	0	$-\frac{2}{3}$	$\frac{2}{3}$	0	$\sqrt{3/8}$
Y	0	1	0	$\frac{1}{6}$	$\frac{1}{3}$	$-\frac{2}{3}$	$-\frac{1}{2}$	1	0	$-\frac{1}{2}$	$\frac{1}{2}$	$-\frac{1}{3}$	$\frac{1}{3}$	0	$\sqrt{3/5}$
P	0	0	1	$\frac{1}{3}$	$\frac{2}{3}$	$\frac{2}{3}$	1	0	0	-1	-1	$-\frac{2}{3}$	$-\frac{4}{3}$	2	$\sqrt{3/20}$
$S^{(1)}$	5	-4	0	1	-3	1	-3	1	5	2	-2	-2	2	0	$\sqrt{1/40}$
$S^{(2)}$	0	2	5	2	4	2	4	2	0	-6	-4	-4	-6	10	$\sqrt{1/160}$
$S^{(3)}$	10	-6	5	4	-2	4	-2	4	10	-2	-8	-8	-2	10	$\sqrt{1/240}$
$S^{(4)}$	0	-2	1	0	0	2	2	-2	0	0	-2	0	-2	2	$\sqrt{1/16}$
$S^{(5)}$	2	6	1	2	2	-4	-4	8	2	-4	2	-4	2	2	$\sqrt{1/96}$
$S^{(6)}$	1	-2	0	0	-1	1	0	-1	1	1	-1	0	0	0	$\sqrt{1/4}$
$S^{(7)}$	3	0	0	1	-1	-1	-3	3	3	0	0	-2	2	0	$\sqrt{1/24}$

$$\psi^{(1),(4),(6),(7)} = \begin{pmatrix} \bar{N} \\ N^c \end{pmatrix}, \quad \psi^{(2),(3),(5)} = \begin{pmatrix} \bar{N} \\ P \end{pmatrix}, \tag{10}$$

where P is some other particle with zero charge under the relevant symmetry.

ψ interacts with a germanium nucleus via a t-channel Z' exchange, as in Fig. 1. The effective Lagrangian is

$$\mathcal{L} = \sqrt{2}G'\bar{\psi}\gamma^\mu(V_\psi - A_\psi\gamma_5)\psi\overline{\mathrm{Ge}}\gamma_\mu(V_{\mathrm{Ge}} - A_{\mathrm{Ge}}\gamma_5)\mathrm{Ge}\ . \tag{11}$$

Here $V_\psi = S_L + S_R$ and $A_\psi = S_L - S_R$, where S_L and S_R are the U(1)′ charges of ψ_L and ψ_R, respectively. V_{Ge} is a sum of constituent charges, so it is of the order of the atomic weight $A = 72.6$. A_{Ge} (the "Gamow-Teller strength") is a sum of spins, so it is of the order of the nuclear spin, which is only nonzero for ^{73}Ge with natural abundance of 7.8%. Thus we can ignore A_{Ge} in our calculations.

The standard-model neutrino interaction (via the Z^0) can be recovered from (11) by

$$\psi \to \nu\ ,\quad G' \to G_F\ ,\quad S_L = \tfrac{1}{2}\ ,\quad S_R = 0\ , \tag{12}$$
$$V_{\mathrm{Ge}} = (\tfrac{1}{2} - 2\sin^2\theta_W)Z - \tfrac{1}{2}N\ ,$$

while in our prototype U(1)′ model we have

$$S_L = S(N^c) = \sqrt{\tfrac{5}{8}}\ ,\quad S_R = -S(N) = 0\ , \tag{13}$$
$$V_{\mathrm{Ge}} = \sqrt{\tfrac{2}{5}}Z + \sqrt{\tfrac{8}{5}}N = 71.6\ .$$

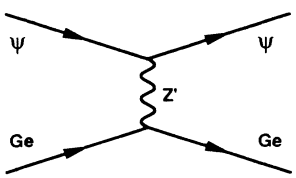

FIG. 1. Interaction with germanium.

In the nonrelativistic limit, σ_{el} is[14]

$$\sigma_{\mathrm{el}} = \frac{2}{\pi}(G'm_\psi V_\psi)^2\left(\frac{M_{\mathrm{Ge}}}{m_\psi + M_{\mathrm{Ge}}}\right)^2 V_{\mathrm{Ge}}^2\ , \tag{14}$$

where $M_{\mathrm{Ge}} = 68\,\mathrm{GeV}$.

A Lee-Weinberg analysis[15] gives the relic abundance of ψ particles from their annihilation cross section σ_A. We assume no particle-antiparticle asymmetry for ψ.[16] Define

$$Z \equiv \sqrt{\frac{45}{4\pi^3 g^*}}m_\psi M_P\langle\sigma_A v\rangle\ ,\quad \langle\sigma_A v\rangle \equiv a + bX_F\ , \tag{15}$$
$$X_F \equiv T_F/m_\psi\ ,$$

where g^* is the effective number of relativistic particle degrees of freedom at the freeze-out temperature T_F. Above 0.2 GeV, g^* approximately obeys[17]

$$g^*(T_F) = 90 - \sqrt{(225\,\mathrm{GeV})/T_F}\ . \tag{16}$$

We set

$$\Omega_\psi = \left(\frac{\ln Z}{Z}\right)\left(\frac{12}{g^*}\frac{1}{2.75}\right)T_0^3 m_\psi/\rho_0 = 1\ . \tag{17}$$

The numerical factors in the second term arise from a depletion in g^*, and a consequent rise in temperature, associated with the QCD phase transition and the electron freeze-out. This gives

$$a + \tfrac{1}{2}bX_F = (9.28\times10^{-10}\,\mathrm{GeV}^{-2})\left(\frac{0.25}{\Omega h_0^2}\right)\sqrt{\frac{90}{g^*}}\left(\frac{\ln Z}{24}\right)\ . \tag{18}$$

Uncertainty in the normalized Hubble parameter h_0 allows $0.16 \le \Omega h_0^2 \le 1$. (If we only require ψ's to constitute the halo, then $0.016 \le \Omega h_0^2 \le 0.1$.) The value $\Omega h_0^2 = \frac{1}{4}$

is preferred on theoretical grounds to close the Universe and give it a sufficient age for stellar evolution.

The annihilation diagram of Fig. 2 in the nonrelativistic limit[14,18] gives

$$\langle \sigma_A v \rangle = \frac{4}{\pi}(G' m_\psi V_\psi)^2 (1 + 2RX_F) \sum_f S_f^2 , \tag{19}$$

where

$$R = \frac{V_\psi^2 + A_\psi^2}{2V_\psi^2} . \tag{20}$$

$R = 1$ in all the models we are considering, and in any case since $X_F = (\ln Z)^{-1} \approx 0.04$, R is unimportant here. The last term in (19) is a sum of U(1)′ charges over all kinematically allowed final states, three generations of standard-model particles except possibly the top quark. In our prototype model, for $m_\psi > m_t$, we have $\left(\sum_f S_f^2\right) = 4.125$.

We put (19) into (18), to find that $(G' m_\psi V_\psi)$ is a constant:

$$(G' m_\psi V_\psi)^2 = \frac{7.0 \times 10^{-10}\,\mathrm{GeV}^{-2}}{\sum_f S_f^2} \times \left(\frac{0.25}{\Omega h_0^2}\right) \sqrt{\frac{90}{g^*}} \left(\frac{\ln Z}{24}\right) \left(\frac{1.04}{1 + RX_F}\right) . \tag{21}$$

Hereafter we will drop the last term, since it differs negligibly from 1. But now (14) gives our final result for the germanium cross section:

$$\sigma_{\mathrm{el}} = (2.15 \times 10^{-10}\ \mathrm{b}) \Phi_d \left(\frac{M_{\mathrm{Ge}}}{m_\psi + M_{\mathrm{Ge}}}\right)^2 \times \left(\frac{0.25}{\Omega h_0^2}\right) \sqrt{\frac{90}{g^*}} \left(\frac{\ln Z}{24}\right) \left(\frac{A}{72.6}\right)^2 . \tag{22}$$

Φ_d is a numerical factor which depends on the U(1)′ symmetry, and on whether m_ψ lies above or below the top quark mass; it is normalized to unity for our prototype $S^{(1)}$ in the region $m_\psi > m_t$:

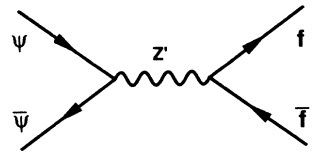

FIG. 2. Annihilation diagram.

$$\Phi_d \equiv 4.24 \frac{(V_{\mathrm{Ge}}/A)^2}{\sum_f S_f^2} . \tag{23}$$

Values of Φ_d for our candidate symmetries appear in Table III [for other U(1)′'s see Appendix A].

Note our result (22) depends only on m_ψ [and the U(1)′ factor Φ_d], not on $M_{Z'}$, g_1', or even V_ψ. A plot of σ_{el} vs m_ψ appears in Fig. 3, for symmetry $S^{(1)}$ and various values of Ωh_0^2. A discontinuity appears at our postulated top-quark mass of 100 GeV; we have chosen not to smooth this out so as to show the effect is small. The experimental limits shown are from a germanium detector,[1] under the assumption that ψ's have the galactic halo density and velocity distribution. In Fig. 4 we have fixed $\Omega h_0^2 = \frac{1}{4}$, and plotted σ_{el} for the seven candidate U(1)′ symmetries listed in Table II.

Equation (21) can be rewritten, using prototype values for V_ψ and $\left(\sum_f S_f^2\right)$, as

$$\frac{(g_1')^2 m_\psi}{M_{Z'}^2} = (9.3 \times 10^{-5}\,\mathrm{GeV}^{-1}) \sqrt{\frac{0.25}{\Omega h_0^2}} . \tag{24}$$

To keep our U(1)′ in the perturbative regime, we take $g_1' < \sqrt{4\pi}$. For a given $M_{Z'}$, this places a lower limit on m_ψ; for example, if $M_{Z'} = 350\,\mathrm{GeV}$ then $m_\psi > 1\,\mathrm{GeV}$.

B. A heavy Dirac fermion

Heavier dark-matter candidates, with $m_\psi \gtrsim \frac{1}{2} M_{Z'}$, require modification of the above calculations, resulting in a germanium cross section which now depends on $M_{Z'}$ and V_ψ. Equation (19) is modified by the pole factor[14]

$$P_{Z'} = \frac{M_{Z'}^4}{(4m_\psi^2 - M_{Z'}^2)^2 + \Gamma_{Z'}^2 M_{Z'}^2} . \tag{25}$$

For $m_\psi > M_{Z'}$ a new annihilation channel opens, $\psi\bar{\psi} \rightarrow$

TABLE III. Multiplicative factors for candidate U(1)′ symmetries.

S	Also known as	$\Phi_d^{(<m_t)}$	$\Phi_d^{(>m_t)}$	Υ_d	$\Phi_m^{(<m_t)}$	$\Phi_m^{(>m_t)}$	Υ_m
$S^{(1)}$	B, χ, Y''	1.0378	1.0000	1.0000	1.0378	1.0000	1.0000
$S^{(2)}$	C, I, Y'	0.1228	0.1146	0.0964	4.4198	4.1250	2.3151
$S^{(3)}$	A, η, Y''', Y_E	0.8362	0.6875	0.6547	0.3716	0.3056	0.2528
$S^{(4)}$	1-flip, $\mathbf{27}, \overline{\mathbf{27}}$	0.5858	0.4882	0.5696	0.0000	0.0000	0.0000
$S^{(5)}$	1-flip, $\mathbf{78}$	0.6590	0.5858	0.7459	1.3751	1.2222	11.3403
$S^{(6)}$	2-flip	0.0034	0.0029	0.0034	2.2918	1.9643	5.5061
$S^{(7)}$	$B - L$	1.3744	1.3038	1.4668	0.0000	0.0000	0.0000

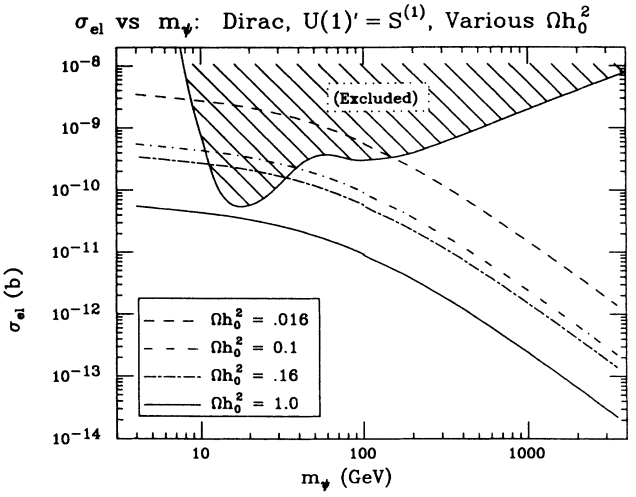

FIG. 3. $\sigma_{\rm el}$ vs m_ψ: Dirac, $S^{(1)}$, various Ωh_0^2. For $m_\psi \ll \frac{1}{2}M_{Z'}$, $\sigma_{\rm el}$ is independent of $M_{Z'}$, g_1', and V_ψ.

$Z'Z'$, from Fig. 5.[19] In the nonrelativistic limit, this contribution is[20]

$$\langle\sigma_A v\rangle_{Z'Z'} = \frac{R^2}{64\pi}\frac{(g_1'V_\psi)^4}{m_\psi^2}\left(\frac{m_\psi(m_\psi^2 - M_{Z'}^2)^{3/2}}{(m_\psi^2 - \frac{1}{2}M_{Z'}^2)^2}\right), \tag{26}$$

where R was defined in (20). Note the last term goes to unity for $m_\psi \gg M_{Z'}$.

We combine Eqs. (19), (25), and (26) to get the total annihilation cross section $\langle\sigma_A v\rangle$, then put this in (18) to get

$$(G'm_\psi V_\psi)^2 = \frac{7.29\times10^{-10}\,\mathrm{GeV}^{-2}}{f_d(m_\psi)}\left(\frac{m_\psi}{M_{Z'}}\right)^4 \times\left(\frac{0.25}{\Omega h_0^2}\right)\sqrt{\frac{90}{g^*}}\left(\frac{\ln Z}{24}\right), \tag{27}$$

where

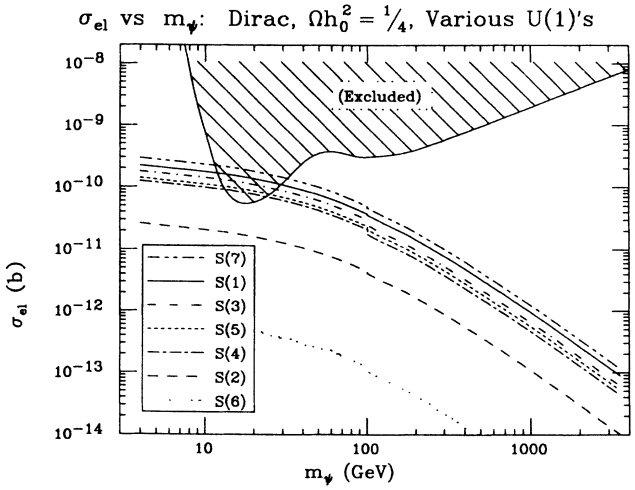

FIG. 4. $\sigma_{\rm el}$ vs m_ψ: Dirac, $\Omega h_0^2 = \frac{1}{4}$, various U(1)′s. $\sigma_{\rm el}$ depends on the U(1)′ only through Φ_d, from Table III.

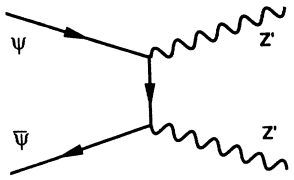

FIG. 5. $\psi\bar\psi \to Z'Z'$.

$$f_d(m_\psi) \equiv \frac{m_\psi^4\left(\sum_f S_f^2\right)(1+RX_F)}{(4m_\psi^2 - M_{Z'}^2)^2 + \Gamma_{Z'}^2 M_{Z'}^2} + \frac{R^2V_\psi^2}{8}\frac{m_\psi(m_\psi^2 - M_{Z'}^2)^{3/2}}{(m_\psi^2 - \frac{1}{2}M_{Z'}^2)^2}. \tag{28}$$

The last term of (28) vanishes for $m_\psi < M_{Z'}$. Note $f_d(m_\psi \gg M_{Z'}) \to 0.346$ (for $S^{(1)}$), and (27) reduces to

$$m_\psi = (3\times10^3\,\mathrm{GeV})(g_1')^2. \tag{29}$$

The requirement $g_1' < \sqrt{4\pi}$ restricts $m_\psi < 40\,\mathrm{TeV}$.

We combine Eqs. (27) and (14) to get $\sigma_{\rm el}$,

$$\sigma_{\rm el} = (1.24\times10^{-11}\ \mathrm{b})\left(\frac{m_\psi}{M_{Z'}}\right)^2\left(\frac{1\,\mathrm{TeV}}{M_{Z'}}\right)^2 \times U_d\Upsilon_d\frac{f_d(\infty)}{f_d(m_\psi)}, \tag{30}$$

where U_d consists of some factors of unity:

$$U_d \equiv \left(\frac{m_\psi}{m_\psi + M_{\rm Ge}}\right)^2\left(\frac{0.25}{\Omega h_0^2}\right)\sqrt{\frac{90}{g^*}}\left(\frac{\ln Z}{24}\right)\left(\frac{A}{72.6}\right)^4. \tag{31}$$

Υ_d is a factor which depends on the U(1)′ symmetry, normalized to unity for $S^{(1)}$, and listed for other symmetries in Table III:

$$\Upsilon_d \equiv 0.356\frac{(V_{\rm Ge}/A)^2}{f_d(\infty)}. \tag{32}$$

Thus, the last three terms of (30) are approximately unity for $m_\psi \gg M_{Z'}$.

Note that we do not include the coherence loss factor η_C,[21] since the experimental limits we quote[1] have already accounted for it.

$\sigma_{\rm el}$ from (30) is plotted against m_ψ for various values of $M_{Z'}$ in Fig. 6. We have used the prototype symmetry $S^{(1)}$, and taken $\Omega h_0^2 = \frac{1}{4}$.

C. A light Majorana fermion

Suppose our prototype model does not contain an N; then in place of Eq. (7) we have a Majorana fermion

$$\psi = \begin{pmatrix}\bar N^c\\ N^c\end{pmatrix}. \tag{33}$$

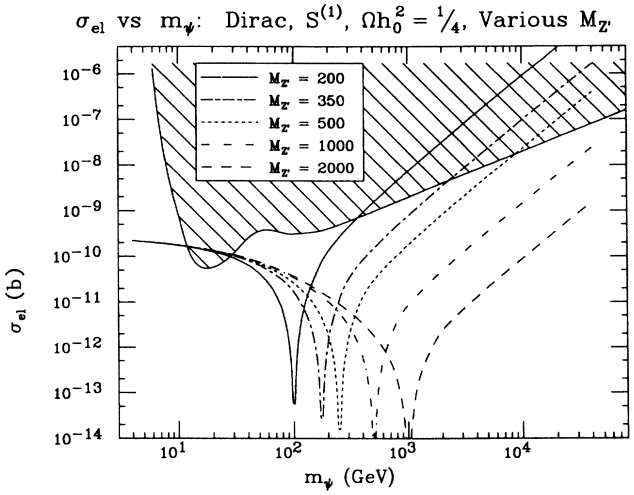

FIG. 6. $\sigma_{\rm el}$ vs m_ψ: Dirac, $S^{(1)}$, $\Omega h_0^2 = \frac{1}{4}$, various $M_{Z'}$. In this range $\sigma_{\rm el}$ depends on $M_{Z'}$.

Then [see (11)] $V_\psi = 0$, $A_\psi = 2S_{N^c}$.[22] In fact, the calculations of this subsection are valid for any fermion with no vector coupling, such as a ψ of the form (7) under symmetries $S^{(3)}$ or $S^{(5)}$.

The germanium cross section is greatly reduced. Equation (14) is replaced by[14]

$$\sigma_{\rm el} = \frac{6}{\pi}(G' m_\psi A_\psi)^2 \left(\frac{M_{\rm Ge}}{m_\psi + M_{\rm Ge}}\right)^2 A_{\rm Ge}^2 \ . \tag{34}$$

We take

$$A_{\rm Ge}^2 = (0.078)(0.37)(S_Q + S_{D^c})^2 \ , \tag{35}$$

where the first numerical term is the relative abundance of ^{73}Ge, and the second is from Table III of Goodman and Witten.[18] Note the axial-vector strength does not scale as the atomic weight. Thus the Majorana cross section is over 5 orders of magnitude smaller than the Dirac case.

The annihilation cross section [compare to (19)] is[14]

$$\langle \sigma_A v \rangle = \frac{4}{\pi}(G' m_\psi A_\psi)^2 X_F \sum_f S_f^2 \ . \tag{36}$$

Combining this with Eqs. (18) and (34) gives $\sigma_{\rm el}$ [compare to (22)]

$$\sigma_{\rm el} = (1.8 \times 10^{-14}\ {\rm b})\Phi_m \left(\frac{M_{\rm Ge}}{m_\psi + M_{\rm Ge}}\right)^2 \times \left(\frac{0.25}{\Omega h_0^2}\right)\sqrt{\frac{90}{g^*}}\left(\frac{\ln Z}{24}\right)^2 \ , \tag{37}$$

$$\Phi_m \equiv 41.3 \frac{(S_Q + S_{D^c})^2}{\sum_f S_f^2} \ . \tag{38}$$

Again, Φ_m is normalized to unity for $S^{(1)}$, and listed for other symmetries in Table III. Equation (37) is plotted for our prototype symmetry, with various values of Ωh_0^2, in Fig. 7. Figure 8 shows $\sigma_{\rm el}$ for our various U(1)′ symmetries, with $\Omega h_0^2 = \frac{1}{4}$ fixed.

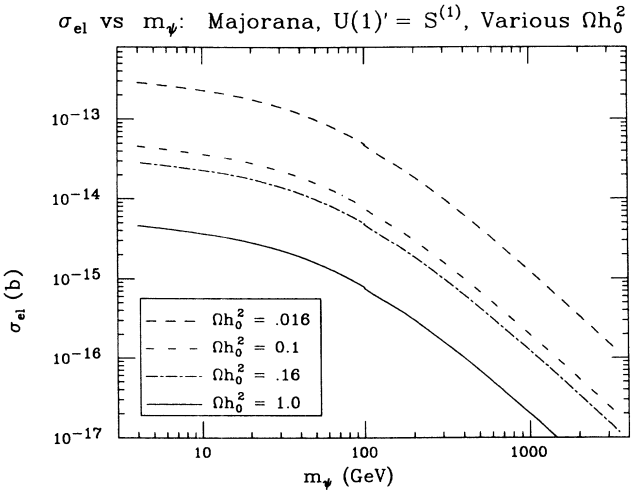

FIG. 7. $\sigma_{\rm el}$ vs m_ψ: Majorana, $S^{(1)}$, various Ωh_0^2. These $\sigma_{\rm el}$'s are experimentally inaccessible.

D. A heavy Majorana fermion

If ψ is Majorana and $m_\psi \gtrsim \frac{1}{2}M_{Z'}$, the annihilation cross section is[20]

$$\langle \sigma_A v \rangle = \frac{4}{\pi}(G' m_\psi A_\psi)^2 \left(\frac{M_{Z'}}{m_\psi}\right)^4 \times \left(\frac{\left(\sum_f S_f^2\right) X_F m_\psi^4}{(4m_\psi^2 - M_{Z'}^2)^2 + \Gamma_{Z'}^2 M_{Z'}^2} + \frac{A_\psi^2}{32}\frac{m_\psi (m_\psi^2 - M_{Z'}^2)^{3/2}}{(m_\psi^2 - \frac{1}{2}M_{Z'}^2)^2} \right) \ . \tag{39}$$

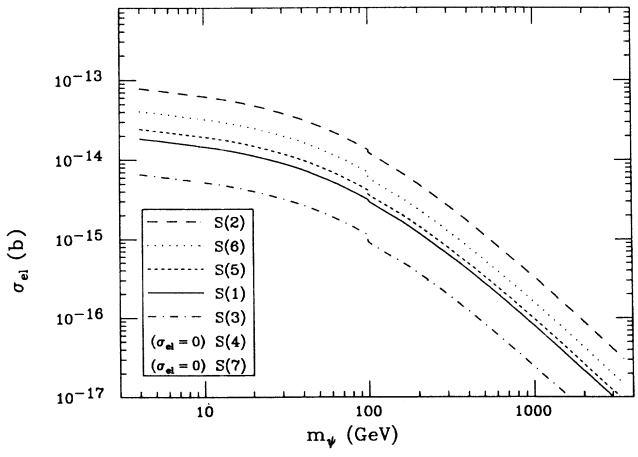

FIG. 8. $\sigma_{\rm el}$ vs m_ψ: Majorana, $\Omega h_0^2 = \frac{1}{4}$, various U(1)′s. $\sigma_{\rm el}$ depends on Φ_m, from Table III.

Then Eqs. (18) and (34) give [compare to (30)]

$$\sigma_{\rm el} = (8.8\times10^{-17}\ {\rm b})\left(\frac{m_\psi}{M_{Z'}}\right)^2\left(\frac{1\,{\rm TeV}}{M_{Z'}}\right)^2 \times U_m \Upsilon_m \frac{f_m(\infty)}{f_m(m_\psi)}\ . \tag{40}$$

Now $f_m(m_\psi)$ is

$$f_m(m_\psi) \equiv \frac{1}{2}\frac{\left(\sum_f S_f^2\right)X_F m_\psi^4}{(4m_\psi^2 - M_{Z'}^2)^2 + \Gamma_{Z'}^2 M_{Z'}^2} + \frac{A_\psi^2}{32}\frac{m_\psi(m_\psi^2 - M_{Z'}^2)^{3/2}}{(m_\psi^2 - \frac{1}{2}M_{Z'}^2)^2} \tag{41}$$

(again the last term vanishes for $m_\psi < M_{Z'}$) and U_m consists of some factors of unity:

$$U_m \equiv \left(\frac{m_\psi}{m_\psi + M_{\rm Ge}}\right)^2\left(\frac{0.25}{\Omega h_0^2}\right)\sqrt{\frac{90}{g^*}}\left(\frac{\ln Z}{24}\right)\left(\frac{A}{72.6}\right)^2\ . \tag{42}$$

Υ_m is a factor which depends on the U(1)′ symmetry, normalized to unity for $S^{(1)}$, and listed for other symmetries in Table III,

$$\Upsilon_m \equiv 0.833\frac{(S_Q + S_{D^c})^2}{f_m(\infty)}\ . \tag{43}$$

The last three terms of (40) are approximately unity for $m_\psi \gg M_{Z'}$.

$\sigma_{\rm el}$ from (40) is plotted against m_ψ for various values of $M_{Z'}$ in Fig. 9. We have used the prototype symmetry $S^{(1)}$, and taken $\Omega h_0^2 = \frac{1}{4}$.

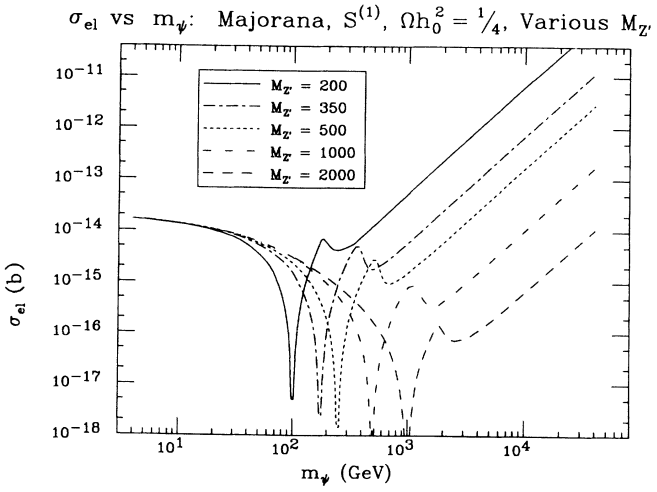

FIG. 9. $\sigma_{\rm el}$ vs m_ψ: Majorana, $S^{(1)}$, $\Omega h_0^2 = \frac{1}{4}$, various $M_{Z'}$.

IV. QUANTUM COMPLICATIONS

Wave-function and mass mixing between the Z and the Z' have been studied extensively in the literature,[9,12,23] especially for our first three candidate symmetries (note, however, that mixing does not occur in all models, e.g., $S^{(7)}$, pure $B-L$). Wave-function mixing, from Fig. 10(a), changes the current to which the Z' couples, slightly altering the Φ and Υ values given in Table III. Mass mixing, from Fig. 10(b), introduces a small coupling of ψ to the 91-GeV gauge-boson mass eigenstate. Measurements of standard-model parameters (such as $\rho = 1$) place limits on the Z' mass and the mixing angle.

Before wave-function renormalization, let the field A_Y couple to J_Y (hypercharge current) and the field A_X couple to J_X. Mixing will cause A_Y to couple to $J_Y + \epsilon J_X$ and A_X to couple to $J_X + \epsilon J_Y$, where $\epsilon \approx (g_1^2/16\pi^2)\ln(M_G/M_{Z'}) \approx 1/20$. The standard-model B field, which couples to J_Y only, must then be

$$B = A_Y - \epsilon A_X \tag{44}$$

and the orthogonal combination, the Z', couples to $J_X + 2\epsilon J_Y$. This changes the ratios λ/β and λ/κ by $O(2\epsilon)$ for the candidate symmetries we listed in Table II.

Mass mixing of the Z and Z' is usually studied under the GUT assumption

$$g_1' = g_1 = \sqrt{\frac{5}{3}}\frac{e}{\cos\theta_W} = 0.46 \tag{45}$$

which is true if $g_1' = g_1$ at the GUT scale and none of the particles in the **27** are heavy. Under these assumptions, and leaving the mixing angle unconstrained, neutral-current data and measurements of the Z and W masses (giving $\rho \approx 1$) place lower limits on $M_{Z'}$. We quote the 90% confidence level limits from Costa *et al.*,[9] using only the constraint $\rho = 1$, for our first three candidate symmetries:

$$\begin{aligned} &M_{Z'} > 352\,{\rm GeV}\ \ (S^{(1)})\ , \\ &M_{Z'} > 180\,{\rm GeV}\ \ (S^{(2)})\ , \\ &M_{Z'} > 129\,{\rm GeV}\ \ (S^{(3)})\ . \end{aligned} \tag{46}$$

From the same source, we find limits on the mass mixing angle $\theta_{\rm mix}$ (in radians):

$$\begin{aligned} &|\theta_{\rm mix}| < 0.05\ \ (S^{(1)})\ , \\ &|\theta_{\rm mix}| < 0.05\ \ (S^{(2)})\ , \\ &|\theta_{\rm mix}| < 0.20\ \ (S^{(3)})\ . \end{aligned} \tag{47}$$

As pointed out by Enqvist et al.,[24] even these small an-

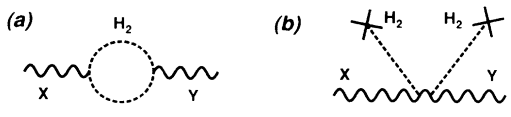

FIG. 10. (a) Wave-function mixing, (b) mass mixing (H_2 is the Higgs doublet).

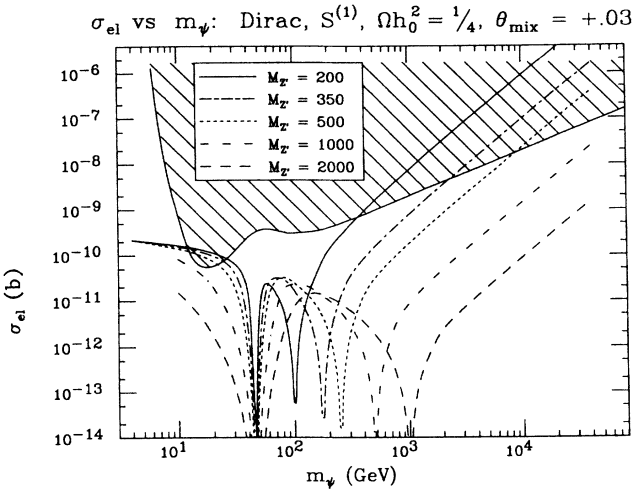

FIG. 11. Figure 6 modified for $\theta_{\rm mix} = 0.03$.

gles can significantly increase $\langle \sigma_A v \rangle$ when $m_\psi \approx M_Z/2$, from the Z^0 resonance. This translates for us into a dip in our plots of $\sigma_{\rm el}$ near $m_\psi = 45\,{\rm GeV}$. In Fig. 11 we show how Fig. 6 is modified for $\theta_{\rm mix} = 0.03$.

V. FIXED COUPLING g_1'

In Sec. III B we plotted $\sigma_{\rm el}$ of a Dirac fermion for several fixed values of $M_{Z'}$. Now we will fix the coupling g_1', and let $M_{Z'}$ adjust to satisfy Eq. (27). In particular, we will pay homage to the GUT's by taking $g_1' = 0.46$, as well as exploring a range around that value. We can also use the $M_{Z'}$ limits of Eq. (47), along with Eq. (24), to put lower limits on m_ψ:[24]

$$\begin{aligned} m_\psi &> 55\,{\rm GeV} \quad (S^{(1)}) , \\ m_\psi &> 20\,{\rm GeV} \quad (S^{(2)}) , \\ m_\psi &> 13\,{\rm GeV} \quad (S^{(3)}) , \end{aligned} \tag{48}$$

where each value should be multiplied by $\sqrt{0.25/\Omega h_0^2}$.

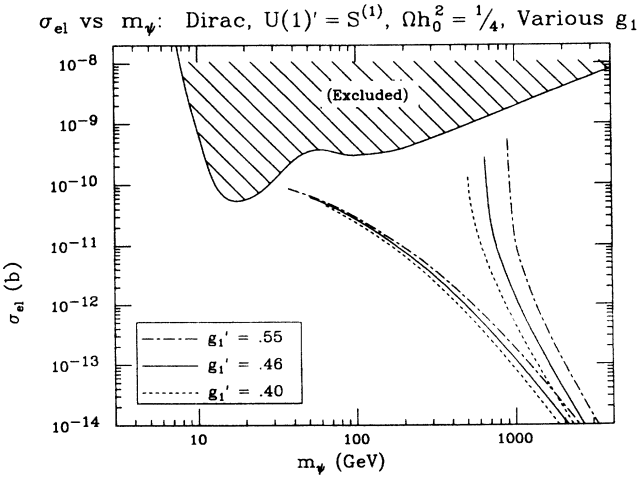

FIG. 12. $\sigma_{\rm el}$ vs m_ψ: Dirac, $S^{(1)}$, $\Omega h_0^2 = \frac{1}{4}$, various g_1'. GUT's which fix g_1' restrict $\sigma_{\rm el}$ and m_ψ to these two branches.

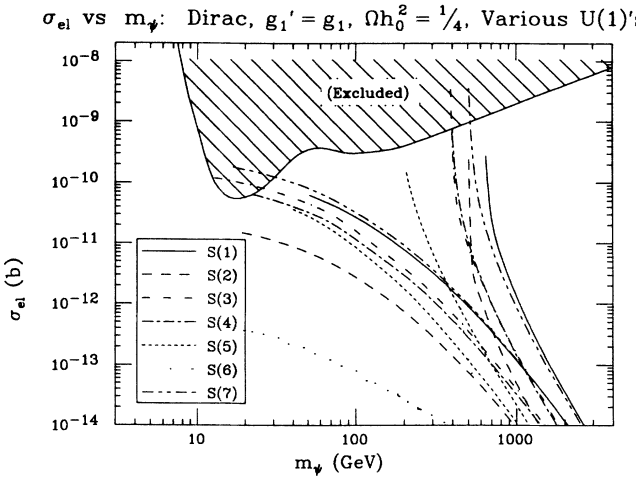

FIG. 13. $\sigma_{\rm el}$ vs m_ψ: Dirac, $g_1' = g_1 = 0.46$, $\Omega h_0^2 = \frac{1}{4}$, various U(1)'s, from GUT's with no intermediate mass scale.

At fixed g_1' and $M_{Z'}$, Eq. (27) has two solutions for m_ψ, one below $\frac{1}{2}M_{Z'}$ and one above. So as we let $M_{Z'}$ vary, we get two branches (the "low" and "high" branches) in our plot of $\sigma_{\rm el}$ vs m_ψ, Fig. 12. The low branch looks similar to Fig. 4 [but with Eq. (48) imposed], since $\sigma_{\rm el}$ is nearly independent of $M_{Z'}$ for $m_\psi \ll M_{Z'}$. The nearly vertical nature of the high branch can be understood from Eq. (29), which shows that for low Z' masses, $m_\psi = 650$ GeV, while from (30) we know $\sigma_{\rm el} \sim 1/M_{Z'}^4$. Lower limits on $M_{Z'}$ in this case translate to upper limits on $\sigma_{\rm el}$.

In Fig. 13 we have superimposed the GUT-constrained cross sections ($g_1' = 0.46$) from all seven of our candidate symmetries. We have arbitrarily taken $M_{Z'} > 180\,{\rm GeV}$ for symmetries 4–7.

VI. CONCLUSIONS

As long as $m_\psi \ll M_{Z'}$, we can predict $\sigma_{\rm el}$ vs m_ψ for a dark-matter U(1)'-coupled Dirac fermion, without knowing any details about the Z' mass, the coupling g_1', or even the fermion charge V_ψ. Uncertainty in the Hubble parameter and in the form of the low-energy U(1)' introduce small uncertainties in $\sigma_{\rm el}$. In this regime, the predicted germanium cross section is close to experimental limits for $10\,{\rm GeV} < m_\psi < 100\,{\rm GeV}$. Predicted cross sections for Majorana fermions are much lower.

Another window of experimental detection opens for $m_\psi > \frac{1}{2}M_{Z'}$, anywhere in the range $400\,{\rm GeV} < m_\psi < 40\,{\rm TeV}$, but now the predicted cross section depends on $M_{Z'}$ (or, equivalently, on g_1'). In Fig. 6 we chose to fix $M_{Z'}$, while in Figs. 12 and 13 we fixed g_1' to be the value predicted by certain GUT's. In the latter case, lower limits on $M_{Z'}$ translate to lower limits on m_ψ and upper limits on $\sigma_{\rm el}$.

Under the fairly general assumptions that the dark matter is a U(1)'-coupled fermion, with no particle-antiparticle asymmetry, and with the local density and velocity distribution of the galactic halo, we have shown that dark-matter detectors can powerfully probe the U(1)' sector.

ACKNOWLEDGMENTS

We wish to thank D. Caldwell for leading us to think about U(1)′ dark matter, and also K. Griest, B. Sadoulet, S. Hsu, and F. Zwirner for helpful conversations. L.H. acknowledges the financial support of the Sloan Foundation and the Presidential Young Investigator's Program. D.B. acknowledges the financial support of the National Science Foundation. This work was supported in part by the Director, Office of Energy Research, Office of High Energy and Nuclear Physics, Division of High Energy Physics of the U.S. Department of Energy under Contract No. DE-AC03-76SF00098 and in part by the National Science Foundation under Grant No. PHY85-15857.

APPENDIX: FORMULAS FOR Φ_d, Υ_d, Φ_m, AND Υ_m

Equations (23), (32), (38), and (43) can be calculated for any U(1)′ symmetry from its β, λ, and κ values using

$$\begin{aligned}
\left(\textstyle\sum_f S_f^2\right)(m_\psi < m_t) &= \tfrac{37}{3}\beta^2 + \tfrac{103}{12}\lambda^2 + \tfrac{43}{3}\kappa^2 \\
&\quad + \tfrac{43}{3}\beta\lambda - \tfrac{46}{3}\beta\kappa - \tfrac{17}{3}\lambda\kappa \ , \\
\left(\textstyle\sum_f S_f^2\right)(m_\psi > m_t) &= 13\beta^2 + 10\lambda^2 + 16\kappa^2 \\
&\quad + 16\beta\lambda - 16\beta\kappa - 8\lambda\kappa \ , \qquad \text{(A1)} \\
V_{\rm Ge}/A &= 2\beta + 0.94\lambda - \kappa \ , \\
V_{\rm Ge}/A &= 2\beta + 0.94\lambda - \kappa \ , \\
S_Q + S_{D^c} &= \tfrac{1}{2}\lambda + \kappa \ . \qquad \text{(A2)}
\end{aligned}$$

The terms V_ψ and A_ψ depend on the form of ψ [see Eq. (10)],

$$\begin{aligned}
\psi = \begin{pmatrix} \bar{N} \\ N^c \end{pmatrix} &: \quad V_\psi = \beta - 2\kappa \ , \\
\psi = \begin{pmatrix} \bar{N} \\ P \end{pmatrix} &: \quad V_\psi = -2\kappa \ , \qquad \text{(A3)} \\
\psi = \begin{pmatrix} \bar{N}^c \\ N^c \end{pmatrix} &: \quad A_\psi = 2\beta \ , \\
\psi = \begin{pmatrix} \bar{N} \\ N \end{pmatrix} &: \quad A_\psi = 4\kappa \ .
\end{aligned}$$

[1] D. O. Caldwell, R. M. Eisberg, D. M. Grumm, M. S. Witherell, B. Sadoulet, F. S. Goulding, and A. R. Smith, Phys. Rev. Lett. **61**, 510 (1988); D. O. Caldwell, R. M. Eisberg, and M. S. Witherell, in *Dark Matter*, proceedings of the XXIIIrd Rencontre de Moriond, Les Arcs, France, 1988, edited by J. Audouze and J. Tran Thanh Van (Editions Frontières, Gif-sur-Yvette, 1988); B. Sadoulet, private communication.

[2] S. P. Ahlen, F. T. Avignone III, R. L. Brodzinski, A. K. Drukier, G. Gelmini, and D. N. Spergel, Phys. Lett. B **195**, 603 (1987).

[3] A. Drukier and L. Stodolsky, Phys. Rev. D **30**, 2295 (1984).

[4] M. B. Green, J. H. Schwarz, and E. Witten, *Superstring Theory* (Cambridge University Press, England, 1987); J. P. Derendinger, L. E. Ibáñez, and H. P. Nilles, Nucl. Phys. **B267**, 365 (1986); E. Witten, *ibid.* **B258**, 75 (1985); S. Hsu, private communication.

[5] In addition to the embeddings of Table I, one can switch $D^c \leftrightarrow B^c$, $L \leftrightarrow H$, and $N^c \leftrightarrow N$. Under this transformation, our symmetries transform as $S^{(1)} \leftrightarrow S^{(2)}$, $S^{(3)} \leftrightarrow S^{(3)}$, $S^{(4)} \leftrightarrow S^{(6)}$, $S^{(5)} \leftrightarrow S^{(5)}$, so we do not find any new candidate symmetries this way.

[6] H. Georgi and S. L. Glashow, Phys. Rev. Lett. **32**, 438 (1974).

[7] A. De Rújula, H. Georgi, and S. L. Glashow, Phys. Rev. Lett. **45**, 413 (1980); S. M. Barr, Phys. Lett. **112B**, 219 (1982); I. Antoniadis, J. Ellis, J. S. Hagelin, and D. V. Nanopoulos, Phys. Lett. B **194**, 231 (1987).

[8] J. Rizos and K. Tamvakis, Phys. Lett. B **212**, 176 (1988).

[9] G. Costa, J. Ellis, G. L. Fogli, D. V. Nanopoulos, and F. Zwirner, Nucl. Phys. **B297**, 244 (1988).

[10] T. G. Rizzo, NASA-Ames Report No. IS-J-3091 (unpublished).

[11] L. E. Ibáñez and J. Mas, Nucl. Phys. **B286**, 107 (1987).

[12] J. Ellis, K. Enqvist, D. V. Nanopoulos, and F. Zwirner, Nucl. Phys. **B276**, 14 (1986); E. Cohen, J. Ellis, K. Enqvist, and D. V. Nanopoulos, Phys. Lett. **165B**,76 (1985).

[13] J. C. Pati and A. Salam, Phys. Rev. D **8**, 1240 (1973).

[14] K. Griest and B. Sadoulet, in *Dark Matter in The Universe*, edited by P. Galeotti and D. Schramm (Kluwer Academic, The Netherlands, 1989).

[15] B. W. Lee and S. Weinberg, Phys. Rev. Lett. **39**, 165 (1977); P. Hut, Phys. Lett. **69B**, 85 (1977); K. Sato and M. Kobayashi, Prog. Theor. Phys. **58**, 1775 (1977); M. I. Vysotskii, A. D. Dolgov, and Ya. B. Zel'dovich, Pis'ma Zh. Eksp. Teor. Fiz. **26**, 200 (1977) [JETP Lett. **26**, 188 (1977)]; D. A. Dicus, E.W. Kolb, and V. L. Teplitz, Phys. Rev. Lett. **39**, 168 (1977); G. L. Kane and I. Kani, Nucl. Phys. **B277**, 525 (1986); E. W. Kolb and K. A. Olive, Phys. Rev. D **33**, 1202 (1986); **34**, 2531 (1986).

[16] An interesting U(1)′ cosmion model is developed by G. G. Ross and G. C. Segrè, Phys. Lett. B **197**, 45 (1987), by allowing a particle-antiparticle asymmetry. Their U(1)′, with $(\beta, \lambda, \kappa) = (2, -2, 1)$, allows for a very light Z' (65 GeV) and a large G'. A large scattering cross section for ψ off of helium provides for capture by the Sun, and solves the solar-neutrino problem. Under our assumption of symmetry, the annihilation cross section would also be large, and these ψ's could not close the Universe. However, asymmetry alters the Lee-Weinberg result, so an asymmetric ψ could

cool the Sun and close the Universe.

[17]K. Olive, D. Schramm, and G. Steigman, Nucl. Phys. **B180[FS2]**, 497 (1981).

[18]M. W. Goodman and E. Witten, Phys. Rev. D **31**, 3059 (1985).

[19]We assume the U(1)′ Higgs field is sufficiently massive to avoid $\psi\bar{\psi} \to \phi\phi$.

[20]The annihilation cross section for $\psi\bar{\psi} \to Z'Z'$ in Eqs. (26) and (39) agrees with a more general calculation done by K. Griest and M. Kamionkowski (unpublished).

[21]K. Griest, Phys. Rev. D **38**, 2357 (1988); K. Freese, J. Frieman, and A. Gould, *ibid.* **37**, 3388 (1988); Kim Griest, private communication. Since the momentum transfer becomes independent of m_ψ for large m_ψ, the coherence factor $\eta_C \to 0.3$ in this limit.

[22]This factor of 2 replaces in a natural way the factor of 4 often put by hand into the cross sections, e.g., in Griest and Sadoulet's Appendix A (Ref. 14).

[23]E. Jenkins, Phys. Lett. **192B**,219 (1987); F. Del Aguila, M. Quirós, and F. Zwirner, Nucl. Phys. **B284**, 530 (1987); **B287**, 419 (1987).

[24]K. Enqvist, K. Kainulainen, and J. Maalampi, Nucl. Phys. **B316**, 456 (1989). Enqvist *et al.* independently derive limits on m_ψ from $M_{Z'}$ limits [our Eq. (48)]. For symmetry $S^{(3)}$, using $M_{Z'} \geq 156\,\mathrm{GeV}$, $\Omega h_0^2 \leq \frac{1}{2}$, and fixed $g_1' = g_1$, they find $m_\psi \geq 17\,\mathrm{GeV}$, which is consistent with our result. They do not consider the cross section in a germanium detector; however, they do examine more carefully the effects of $Z^0 - Z'$ mixing, and they have a good discussion of solar capture. We thank K. Griest for pointing this work out to us.